

# SCOUR AT THE TOE OF ROCK ARMoured STRUCTURES

Joost P. den Bieman<sup>1</sup>, Niels G. Jacobsen<sup>1</sup>, Marcel R.A. van Gent<sup>1</sup>

In this work, a CFD model (OpenFOAM) is extended to allow for the exchange of sediment between the inside of porous structures and the outside. This exploratory extended model is applied to simulate the morphological change around and under toe structures, as are often used in rock armoured coastal structures. Both the dimensions of the toe structure and the hydraulic loading are varied to investigate their effect on the simulated scour.

*Keywords: toe structures; scour; OpenFOAM*

## INTRODUCTION

The toe structure of a rock armoured structure provides support to the armour layer and protects the structure from damage due to scour at the toe. Research into the stability of the toe structure itself is readily available. For instance, in Van Gent and Van der Werf (2014) guidelines are provided on the stability of traditional toe structures (see Figure 1). However, in addition to the stability of the stones comprising the toe structure, scour in front of and underneath the structure is relevant for the overall structural integrity of both the toe and armour layer as well. Limited information is available on the processes that affect potential scour near permeable toe structures of rock armoured structures. The numerical model by Jacobsen et al. (2017) models the erosion and accretion of sand within a permeable structure under wave loading. In this work, the Jacobsen et al. (2017) model is extended to deal with transport of sand from outside the permeable structure to inside the structure, and vice versa. The extended model is applied to analyze the scour at the toe of rock armoured structures for toe structures where stones are placed directly on the sandy seabed. Being able to accurately simulate scour nearby and under toe structures would make for a very useful design tool. If the tool indicates that the toe structure can be constructed without a geotextile or without a filter layer, this could lead to a more economical design of the toe structure.

## PROBLEM DEFINITION

For the toe structure to fulfill its purpose of supporting the armour layer and protecting the rest of the structure from scour, it is important for the toe structure itself not to be undermined by scour. However, literature and especially experimental work on the subject is limited. One of the few examples is the experiments by Sumer and Fredsøe (2000), looking at scour at breakwaters, but that work does not contain the scour that occurs underneath the stones. Additionally, there are currently no numerical models that are able to predict this type of scour.

These limitations in both literature and predictive capability of numerical models lead, understandably, to conservatism in design. In practice, often either a filter layer or a geotextile is applied underneath the toe structure to protect against scour. The construction of such a filter layer is costly, so having a tool to predict toe scour to gauge the necessity of a filter layer underneath the toe is valuable.

## NUMERICAL MODEL EXTENSION

Jacobsen et al. (2017) has previously extended OpenFOAM (version foam-extend-3.1) to allow for sediment transport within a porous layer. To this end, a bed-load type sediment transport formula was developed for use inside the porous structure. Jacobsen et al. (2017) excluded a turbulence model, so suspended sediment transport cannot be modelled, and they explain how the effect of suspended sediment transport is incorporated in the bed-load transport formulation. The phase lag between the water movement and sediment transport - typical for suspended sediment - is neglected. The sediment transport is calibrated with experimental data for sedimentation and erosion inside open filters. In this paper, the same sediment transport formula is used inside of porous layers, see Equation 1 and Equation 2 for sediment transport and mobility respectively. In these formulae,  $q_b$  is the bed-load sediment transport,  $C_1$  is a calibration constant,  $\Psi$  is the mobility parameter,  $\Psi_{cr}$  is the critical mobility parameter,  $u_b$  is the near-bed velocity,  $\rho$  is the density of the water,  $\rho_s$  is the density of the sediment,  $s$  is the submerged density of the sediment,  $g$  is the gravitational constant and  $d$  is the water depth. Inside the structure,  $\Psi_{cr,in} = 0.13$  and  $C_1 = 10^{-5}$  is used.

---

<sup>1</sup>Deltares, Delft, The Netherlands. Joost.denBieman@deltares.nl; Niels.Jacobsen@deltares.nl; Marcel.vanGent@deltares.nl

$$q_b = C_1(\Psi - \Psi_{cr})^{1.5} \frac{u_b}{|u_b|} \quad (1)$$

$$\Psi = \frac{\rho|u_b|^2}{(\rho_s - \rho)gd} = \frac{|u_b|^2}{(s - 1)gd} \quad (2)$$

Sediment can now also be exchanged between the porous layer and the outside of the structure. In this exchange, the porosity of the porous layer is accounted for. On the interface of the porous layer and the outside, sediment transport is weighted according to the volumetric portions of the layer within a computational cell.

Outside of the structure, the bed-load sediment transport formula from Ribberink (1998) is applied (recast into mobility parameter form). The following formulae are presented below: sediment transport (Equation 3), mobility number (Equation 4), and critical mobility (Equation 5). In these formulae,  $\Psi_b$  is the bed-load mobility,  $\theta_c$  is the critical Shield parameter,  $f_w$  is the friction factor for waves,  $\alpha$  is the orbital amplitude and  $k_N$  is the Nikuradse roughness height. Outside the structure,  $\Psi_{cr,out} = 11.95$  is used.

$$\Psi_b = m(1/2f_w)^n(\Psi - \Psi_{cr})^n \frac{u_b}{|u_b|}; m = 11; n = 1.65 \quad (3)$$

$$\Psi = \frac{\rho|u_b|^2}{(\rho_s - \rho)gd} = \frac{|u_b|^2}{(s - 1)gd} \quad (4)$$

$$\theta_c = \frac{1/2f_w u_b^2}{(s - 1)gd} = 1/2f_w \Psi_{cr}; f_w = 0.04 \left( \frac{\alpha}{k_N} \right)^{-1/4} \quad (5)$$

The open filter functionality described by Jacobsen et al. (2017) remains fully intact with the recent model extension.

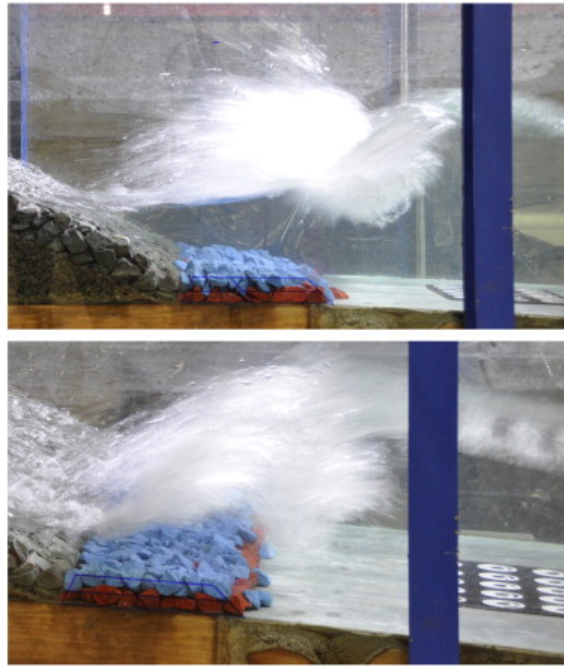


**Figure 1: Example of a traditional toe structure in a physical model under wave loading, from Van Gent and Van der Werf (2014).**

## APPLICATION TO TOE STRUCTURES

The extended numerical model is applied to analyze toe scour. The model setup features a rock armoured structure including a toe structure placed directly on the sandy seabed, which is subjected to wave load. The width and height of the toe structure is varied, as well as the water depth in front of the structure and the wave steepness.

Additionally, one of the tests described by Sumer and Fredsøe (2000) is used for the validation of scour in front of a porous structure.

### Numerical setup

The waves2Foam toolbox for OpenFOAM (Jacobsen et al., 2012) is used for the generation of waves. This method requires the presence of relaxation zones both for the generation of incident and the absorption of reflected waves. The specified incident wave spectrum is composed of linear superimposed frequencies, which are distributed to have a higher frequency around the spectrum peak as opposed to the tails. For the wave forcing in this work, irregular waves are prescribed by JONSWAP spectra with a peak enhancement factor of 3.3. The hydraulic forcing conditions are varied through water level, wave height and wave steepness. An overview of all simulations is given in Table 1. The model runs for 500 waves (based on the  $T_{m-1,0}$ ). A morphological acceleration factor of 5 is applied, so the simulation represents the morphological effect of 2500 waves.

The length of the model domain is 16.3 m, including a relaxation zone on the offshore side with a length of 7.0 m. The cell size of the background mesh is about 1.5 cm in all directions, with refinement along the structure and the bottom.

**Table 1: Overview of model runs.**

Name	Toe	$h$ [m]	$H_{m0}$ [m]	$T_p$ [s]	$s_{0,p}$ [%]
h0w0d050s0015	H0W0	0.50	0.15	4.59	1.5
h0w0d085s0015	H0W0	0.85	0.15	3.62	1.5
h2w3d050s0015	H2W3	0.50	0.15	4.59	1.5
h2w3d085s0015	H2W3	0.85	0.15	3.62	1.5
h3w3d050s0015	H3W3	0.50	0.15	4.59	1.5
h3w3d050s0025	H3W3	0.50	0.15	2.83	2.5
h3w3d050s0040	H3W3	0.50	0.15	1.87	4.0
h3w3d085s0015	H3W3	0.85	0.15	3.62	1.5
h3w3d085s0025	H3W3	0.85	0.15	2.32	2.5
h3w3d085s0040	H3W3	0.85	0.15	1.64	4.0
h4w3d050s0015	H4W3	0.50	0.15	4.59	1.5
h4w3d085s0015	H4W3	0.85	0.15	3.62	1.5
h3w6d050s0015	H3W6	0.50	0.15	4.59	1.5
h3w6d085s0015	H3W6	0.85	0.15	3.62	1.5

### Model setup

The simulated structure has a slope of 1:2 and consists of an impermeable core, covered by a rock armour layer ( $D_{n,50} = 5$  cm) with variations on a toe structure. These variations differ in toe width and height, and are displayed in Figure 2. The structure is placed directly on top of a horizontal mobile sand layer. Both the rock armour layer and the core are, however, immobile. Additionally, the structure has a porosity of 0.4 and resistance coefficients  $\alpha = 1000$  and  $\beta = 1.1$ .

The results of the model runs are presented in the following sections, with special attention to the influence of the different hydraulic load parameters, the toe structure layout, and the temporal development of the scour hole.

### Influence of hydraulic load

The hydraulic load on the structure is varied through both changing the water level and the wave steepness, using a constant wave height and varying wave period (see Table 1). In all cases, the same toe structure is used: H3W3 layout (both toe width and height equal to 3 stone diameters).

The final bed level for the hydraulic load variations is presented in Figure 3 for two different water

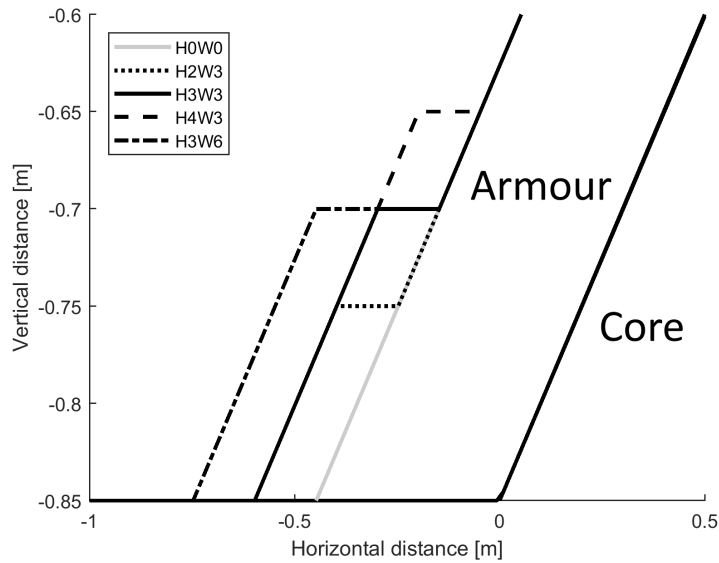


**Figure 2: Different configurations of the toe structure.**

depths, including the outline of the structure. The depicted simulations feature the same wave height (0.15 m) with different wave steepness (1.5%, 2.5% and 4%) and water depth (0.50 m and 0.85 m). When comparing Figure 3a to Figure 3b, the influence of the water level becomes apparent: the lower water level leads to more morphological change. Similarly, the smaller the wave steepness (thus the longer the waves) the more morphological change is predicted. Both are consistent with larger wave orbital velocities near the interface between the toe structure and the sandy bottom.

For all results, the pattern is fairly similar. Firstly, a scour hole forms exactly at the interface between the inside and outside of the toe structure. Secondly, there is sedimentation inside the toe structure itself. In some cases this almost leads to complete infilling of the toe structure itself. Finally, the combination of low steepness and small water depth causes a larger scale undulating pattern, stretching out offshore from the structure for several meters (not shown).

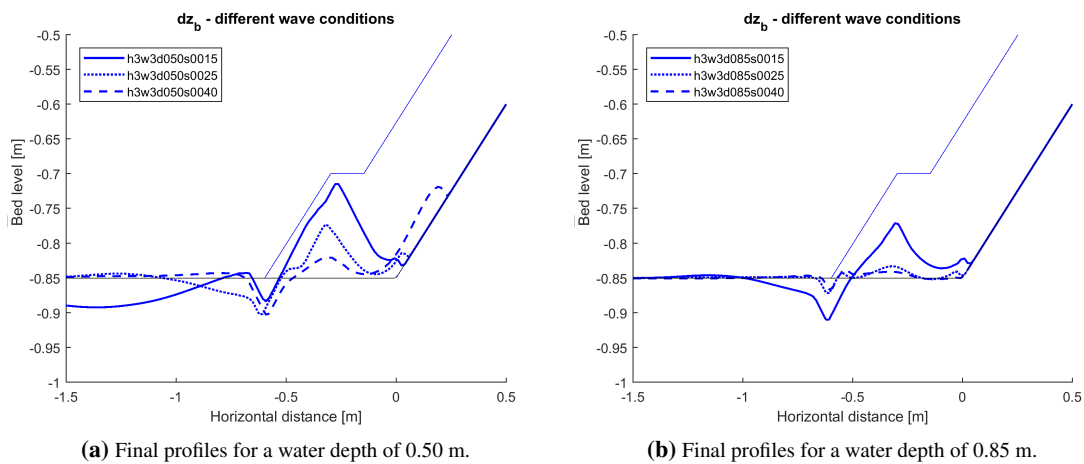


**Figure 3: Influence of wave conditions. Legend names match run names in Table 1.**

### Influence of toe structure layout

The layout of the toe structure has been varied in either the width or the height (see Table 1). The hydraulic conditions are kept constant with a wave height of 0.15 m, peak period of 4.59 s and a wave steepness of 1.5%. In Figure 4, the height of the toe structure is varied between 2, 3 and 4 stone diameters ( $D_{n,50} = 5$  cm). conversely, in Figure 5 the toe width is varied between 3 and 6 stone diameters.

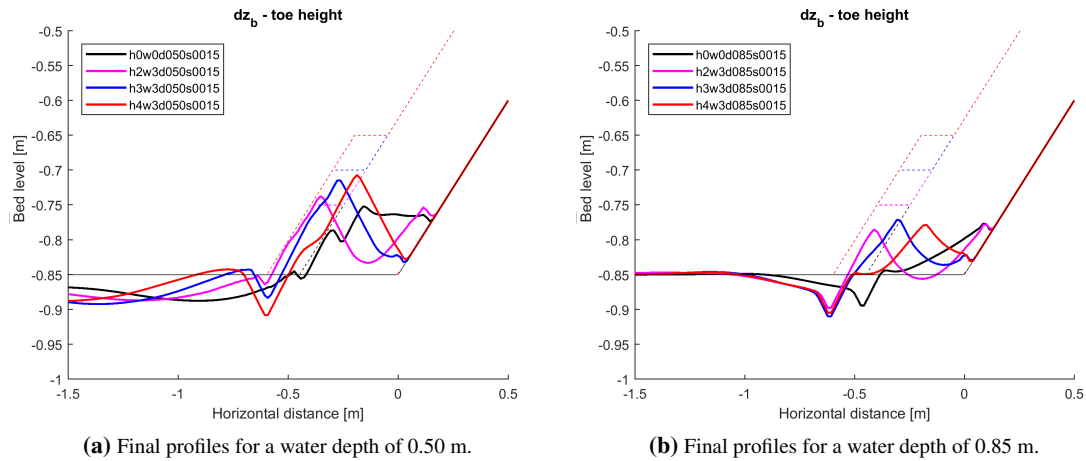


**Figure 4: Influence of toe height. Legend names match run names in Table 1.**

Increasing the height of the toe structure (see Figure 4) primarily affects the sedimentation pattern inside. The crest of the sedimentation appears to move outward with an increasing crest height of the toe structure. In one of the cases, the sedimentation height even slightly exceeds the height of the toe structure itself. Additionally, for the cases with the smaller water depth, the final depth of the scour hole at the stone/sand interface is also dependent on the height of the toe structure: the higher the toe structure, the deeper the scour hole.

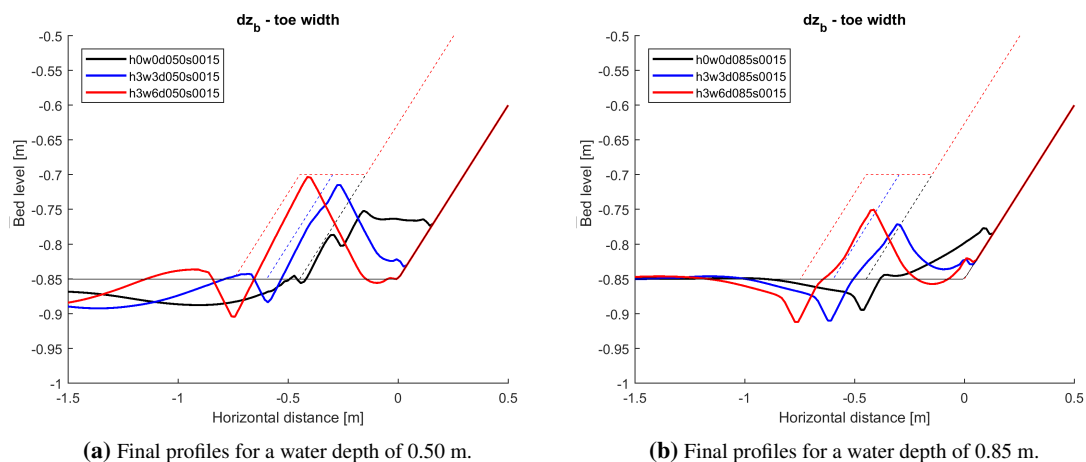


**Figure 5: Influence of toe width. Legend names match run names in Table 1.**

Increasing the width of the toe structure (see Figure 5) shows a very similar pattern, shifted slightly in offshore direction. The absence of the toe structure still leads to sedimentation inside the rock armour layer itself against the core material. Not only the sedimentation pattern inside of the structure shifts, also the larger undulating pattern outside of the structure shifts horizontally.

### Scour hole development

One of the shared features in Figure 3 to Figure 5 is the scour hole that occurs right at the interface of the sandy bed and the toe structure. When looking at the development of this scour hole over time, roughly three different behaviours can be distinguished: progressive scour, stabilizing scour and infilling of the scour hole. Examples of the different behaviors are shown in Figure 6.

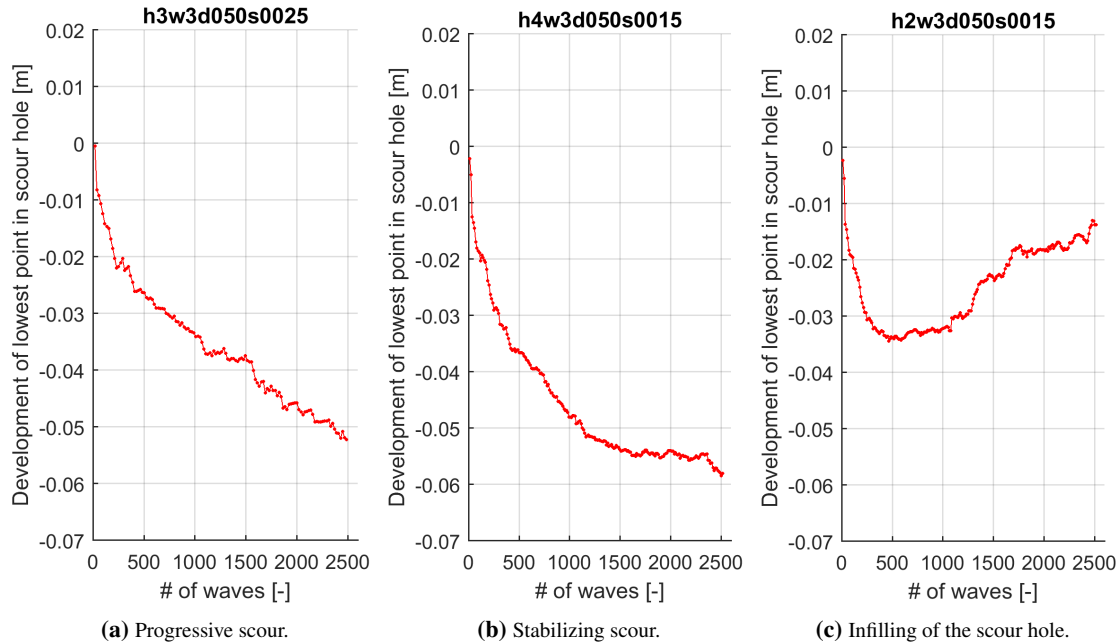


**Figure 6: Different temporal behaviors of scour development. Figure names match run names in Table 1.**

In case of progressive scour (Figure 6a) the depth of the scour hole increases in time. This means that not all cases reach an equilibrium state within the simulated morphological development of 2500 waves. With stabilizing scour (Figure 6b), the depth of the scour hole does not increase or decrease anymore, suggesting that an equilibrium situation was reached. While with infilling of the scour hole (Figure 6c), the depth of the scour hole first increases, then stabilizes and finally starts to decrease again. The source of the sand moving into the scour hole seems to be the infilling of almost the entire seaward side of the toe structure. This eventually causes avalanching sand (the avalanching mechanism is present in the model) to move into the scour hole, reducing it in depth (for instance, see the pink line in Figure 4a).

Additionally, the observed behavior is of course dependent on the number of simulated waves. For instance, would the simulation in Figure 6c have stopped after about 600 waves, the observed behavior would be stabilizing scour, instead of infilling. Similarly, if the number of simulated waves is increased progressive scour can stabilize and the scour hole might fill in again. A continued scour prediction was not attempted in this study.

### Validation scour in front of structure

As mentioned before, . In exploratory testing, one of the physical model tests from Sumer and Fredsøe (2000) is also simulated. This is no strict validation of the bed level change inside the structure, as Sumer and Fredsøe (2000) only provide data on the scour in front of the structure. Hence, Test 17 is used as a validation case for the scour in front of the structure. This test features a breakwater structure with a slope of 1:1.2. The hydraulic conditions used are  $H_s = 0.136$  m and  $T_p = 1.9$  s with a water depth of 0.31 m.

As can be seen from Figure 7, the model results do not matched the observed bed level change well. In the model, there are large amounts of accretion inside the structure, and a scour hole somewhat removed from it. While in the measurements the observed scour hole is located closer to the structure. Additionally, a pronounced undulating pattern of erosion and accretion is measured in the physical model, that is not reproduced by the numerical model.

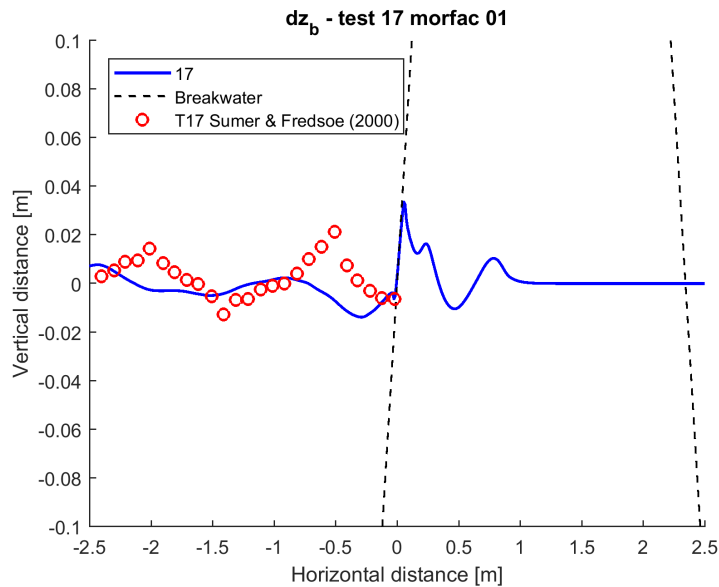


**Figure 7: Validation results for test 17 reported in Sumer and Fredsøe (2000) with model results (blue line), measurements (red circle) and breakwater geometry (black dashed line).**

However, Figure 7 mention that the sand bed was covered by ripples. This opens up the possibility of the reversion of the direction of sediment transport, by the vortex generation over the ripples and the subsequent importance of suspended sediment transport. These processes are not included in the numerical model.

## DISCUSSION

As can be gathered from the above, all modelled cases lead to a mound of accreted material inside of the toe structure, regardless of the structure layout of the hydraulic forcing applied. This is surprising for multiple reasons. Firstly the assumption was that using a bed-load transport only sediment transport formula would be conservative. This is because, in the idealized vertical wall case Gislason et al. (2009) describes, the bed-load sediment transport gradients are large near the structure. If this is indeed the case that would imply that including suspended transport would result in even less erosion or more accretion. This seems unrealistic, given the large amounts of accretion already modelled.

There is a smaller scour hole at the interface between the toe structure and the outside. This scour hole seems unrealistically narrow, with slopes virtually equal to the angle of repose. This suggests that the erosion is very much concentrated exactly at the interface, with the adjacent sediment avalanching in the scour hole when the slope becomes too steep.

Looking at the morphological development outside of the structure, the largest scour hole is actually some distance removed from the structure itself. The trough of the larger scale scour hole is located some distance away. This is part of a larger scale sedimentation and erosion pattern, which seemingly has a node at the toe itself, with the scour hole (anti-node) some way removed. Keep in mind however that the model was shown to be unable to reproduce scour in front of the structure in the validation case.

When interpreting these simulation results, one has to bear in mind that the underlying sediment transport formulation has two inherent assumptions. Firstly, it is a bed load sediment transport formulation, thus assuming that any suspended sediment transport does not have a significantly large influence on the net sediment transport compared to the bed load component. Conversely, conditions where one would normally expect bed-load sediment transport may well lead to suspension of sediment within of the porous layer because of the different water motion inside. If suspended transport is indeed an important factor, then both the diffusion of suspended sediment and the phase lag between hydrodynamics and sediment transport become of significant importance. Both require a turbulence model inside of the porous layer and a recalibration of the sediment transport formula.

Secondly, this sediment transport formulation has been calibrated by Jacobsen et al. (2017) for use in sloped open filter constructions, looking at the morphological changes on the underlying slope. These morphological changes take place approximately around the water line. In contrast, the area of interest in this work is the bed level change around the toe construction, and thus located at the bottom of the water column. Both of the aspects above make for reasons that the sediment transport formulation used might not necessarily be well suited to describe the physical phenomenon of interest; toe scour. Additionally, in the numerical model there is a very large change in porosity, from the outside (completely 'porous') to the porosity inside the structure. In reality, there is a gradient of increasing porosity towards the inside of the structure, i.e.; the most outward stones are protruding somewhat from the structure, creating a smoother transition in porosity than is modelled numerically. This may well reflect on the observed morphological development, especially at the interface between inside and outside the structure.

Ultimately, the predictive capabilities of this model extension need to be shown by comparison with validation data. The authors are not aware of any such data having been published, featuring toe constructions in different configurations and measurements of the sand bed underneath the structure. Hence, such toe scour tests have since been performed at Deltares. However, the results of which are yet to be published at the time of writing. Initial observations suggest that suspended sediment transport plays a role inside the structure for conditions that would be classified as bed-load only.

### **CONCLUSIONS AND RECOMMENDATIONS**

This paper describes the extension of the OpenFOAM numerical model to allow for exchange of sediment between the inside and outside of porous structures. This new feature has been demonstrated by an exploratory application to different toe scour cases. These cases show the sensitivity of the predicted morphological development to the hydraulic forcing conditions and toe structure dimensions. The resulting sedimentation and erosion patterns are remarkable: the significant sedimentation inside of the toe structure is contrary to expectation, especially since it seems to take place in virtually all cases. Also the scour hole on the interface of structure and sand looks unrealistically narrow.

These interpretations of the results are not yet based on a comparison with validation data of bed level change inside the porous structure. When the data from the Deltares toe scour tests has been published and becomes available for validation, the morphological development inside the structure can be properly assessed. From initial observations from these physical model tests, suspended sediment transport does play a role inside the structure. This leads to doubts with regards to the assumption of only bed load transport in the sediment transport equations.

### **ACKNOWLEDGMENTS**

This research was carried out as part of the Joint Industry Project JIP CoastalFoam. The co-funding by TKI Dynamics of Hydraulic Structures (Delta Technology) is also acknowledged.

**References**

- Gislason, K., Fredsøe, J., and Sumer, B. M. (2009). Flow under standing waves: Part 2. scour and deposition in front of breakwaters. *Coastal Engineering*, 56(3):363 – 370.
- Jacobsen, N. G., Fuhrman, D. R., and Fredsøe, J. (2012). A wave generation toolbox for the open-source CFD library: Openfoam®. *International Journal for Numerical Methods in Fluids*, 70(9):1073–1088.
- Jacobsen, N. G., Van Gent, M. R. A., and Fredsøe, J. (2017). Numerical modelling of the erosion and deposition of sand inside a filter layer. *Coastal Engineering*, 120:47 – 63.
- Ribberink, J. S. (1998). Bed-load transport for steady flows and unsteady oscillatory flows. *Coastal Engineering*, 34(1):59 – 82.
- Sumer, B. M. and Fredsøe, J. (2000). Experimental study of 2D scour and its protection at a rubble-mound breakwater. *Coastal Engineering*, 40(1):59 – 87.
- Van Gent, M. R. A. and Van der Werf, I. M. (2014). Rock toe stability of rubble mound breakwaters. *Coastal Engineering*, 83:166 – 176.